Amino Acids (2011) 40:641–651
DOI 10.1007/s00726-010-0691-3

ORIGINAL ARTICLE

A proteomic analysis of PKCε targets in astrocytes: implications for astrogliosis

Miguel Burgos · Noelia Fradejas · Soledad Calvo · Sung Ung Kang · Pedro Tranque · Gert Lubec

Received: 1 July 2010 / Accepted: 6 July 2010 / Published online: 17 July 2010

Abstract Astrocytes are glial cells in the central nervous system (CNS) that play key roles in brain physiology, controlling processes, such as neurogenesis, brain energy metabolism and synaptic transmission. Recently, immune functions have also been demonstrated in astrocytes, influencing neuronal survival in the course of neuroinflammatory pathologies. In this regard, PKCepsilon (PKCε) is a protein kinase with an outstanding role in inflammation. Our previous findings indicating that PKCε regulates voltage-dependent calcium channels as well as morphological stellation imply that this kinase controls multiple signalling pathways within astrocytes, including those implicated in activation of immune functions. The present study applies proteomics to investigate new protein targets of PKCε in astrocytes. Primary astrocyte cultures infected with an adenovirus that expresses constitutively active PKCε were compared with infection controls. Two-dimensional gel electrophoresis clearly detected 549 spots in cultured astrocytes, and analysis of differential protein expression revealed 18 spots regulated by PKCε. Protein identification by mass spectrometry (nano-LC–ESI-MS/MS) showed that PKCε targets molecules with heterogeneous functions, including chaperones, cytoskeletal components and proteins implicated in metabolism and signalling. These results support the notion that PKCε is involved in astrocyte activation; also suggesting that multiple astrocyte-dependent processes are regulated by PKCε, including those associated to neuroinflammation.

Keywords Neuroinflammation · Glia · Reactive astrocytes · Chaperone · α-B-crystallin · HSP60 · Protein kinase

Introduction

Astrocytes, the most abundant non-neuronal cell type in the central nervous system (CNS), represent approximately half of the volume of the adult mammalian brain (Agulhon et al. 2008). Although originally considered as structural elements, the fact is that the functional diversity of these cells is astonishing. Thus, astrocytes involved in guidance of migrating neurons in early development (Rakic 1972), are essential for the maintenance of the blood brain barrier (Abbott et al. 1992) and provide structural and metabolic support for neurons (Brown and Ransom 2007; Tsacopoulos and Magistretti 1996). They also influence neurotransmission by controlling extracellular glutamate levels as well as the concentration of ions, such as K^+ (Hertz et al. 1999; Karwoski et al. 1989).

In addition, astrocytes along with microglia are responsible for innate neuroimmunity, so that activation of astrocytes (reactive astrogliosis) is a hallmark of the neuroinflammatory processes associated to diverse neuropathologies (Buffo et al. 2010; Dong and Benveniste 2001; Skaper 2007). Therefore, astrocytes assume critical roles in disorders, such as epilepsy, trauma, ischemic stroke, Alzheimer's and Parkinson's diseases and amyotrophic

Electronic supplementary material The online version of this article (doi:10.1007/s00726-010-0691-3) contains supplementary material, which is available to authorized users.

M. Burgos · S. U. Kang · G. Lubec (✉)
Department of Pediatrics, Medical University of Vienna, Währinger Gürtel 18-20, 1090 Vienna, Austria
e-mail: gert.lubec@meduniwien.ac.at

M. Burgos · N. Fradejas · S. Calvo · P. Tranque
Departamento de Ciencias Médicas, Instituto de Investigación en Discapacidades Neurológicas (IDINE), Universidad de Castilla-La Mancha, Albacete, Spain

lateral sclerosis (Blasko et al. 2004; Giaume et al. 2007; Maragakis and Rothstein 2006). Interestingly, astrocytes undergo a remarkable transformation to become reactive. This includes hypertrophy, extension of cell processes and secretion of cytokines and other inflammatory mediators. Relative to the functional consequences of astrocyte activation, mounting evidence demonstrates that reactive astrocytes can contribute to neuroinflammation and exacerbate brain injury (Laird et al. 2008). Accordingly, reactive astrocytes present in the glial scar formed in focal brain lesions inhibit axonal growth and represent a barrier to regeneration (Rolls et al. 2009). Nevertheless, also a growing number of reports sustain that reactive astrocytes play multiple beneficial roles on neuronal survival in neuropathology (Bush et al. 1999; Faulkner et al. 2004).

On the other hand, PKCε is a novel PKC isoform (phorbol ester-sensitive and Ca^{2+}-insensitive) that controls cell shape, growth and differentiation in several cell types (Akita 2002). Interestingly, it is also implicated in the regulation of inflammatory processes in a variety of tissues (Aksoy et al. 2004; Castrillo et al. 2001; Tan and Parker 2003) including CNS (Premkumar and Ahern 2000; Wang et al. 2004). Our previous work provides data supporting the involvement of PKCε in the acquisition of a reactive morphology in astrocytes in response to proinflammatory agents, such as lipopolysaccharide (LPS; Burgos et al. 2007a). We also found that PKCε upregulates voltage-gated calcium channels (Burgos et al. 2007b), known to increase in reactive astrocytes in brain trauma and ischemia models (Chung et al. 2001; Westenbroek et al. 1998). These latest observations imply that a vast number of calcium-dependent processes may be controlled by PKCε in these cells. In conclusion, PKCε is likely to contribute to brain inflammation through the regulation of signalling cascades leading to astrocyte activation.

Proteomic technology has been successfully applied to investigate astrocyte biology. Among other applications, proteomics has enabled recognition of molecules mediating transformation of astrocytes to a reactive phenotype by endothelin-1 (Egnaczyk et al. 2003), characterization of secreted proteins (Dowell et al. 2009; Keene et al. 2009), analysis of responses to morphine (Suder et al. 2009) and effects of ageing (Diez-Vives et al. 2009). In our hands, proteomics has also proven a powerful method for identification of cytoskeleton, signalling, metabolic, antioxidant and proteasomal proteins in different cell types including astrocytes (Myung et al. 2009; Peyrl et al. 2003; Yang et al. 2005). The present study examines the effects of PKCε on the astrocyte proteome. With this purpose, primary astrocyte cultures in which PKCε was adenovirally overexpressed were evaluated using two-dimensional gel electrophoresis (2DE) coupled with mass spectrometry (nano-LC–ESI-MS/MS). Results are discussed in the context of astrocyte reactivity in neuroinflammatory pathologies.

Materials and methods

Animals and primary astrocyte cultures

C57BL/6 mice were maintained in the animal facility at the Albacete Medical School. Cell culture procedures from mice complied with European Union guidelines for the care and use of laboratory animals (council directive 86/609EEC). Primary astrocyte cultures were established from cortex as described (Perez-Ortiz et al. 2004). Briefly, the cerebral hemispheres were aseptically removed from newborn animals (2–4 days old) after decapitation, and cortices were incubated in trypsin–EDTA for 5–10 min at 37°C. Tissue was then mechanically dissociated and resuspended in Dulbecco's modified Eagle's medium containing 10% foetal bovine serum and antibiotics. Cells were grown in 150 cm^2 culture flasks for 12–14 days. The purity of astrocyte cultures was increased by shaking overnight before subculturing.

Adenoviral infection

A replication-defective adenoviral vector driving the expression of constitutively active PKCε (AdCA-PKCε) was obtained from Samarel (Heidkamp et al. 2001). Rat PKCε was rendered constitutively active by deletion of residues 154–163, which correspond to the inhibitory pseudosubstrate domain. Control cultures were infected with adenovirus expressing β-galactosidase (Adβ-GAL) (a gift from A. Samarel) or green fluorescent protein (AdGFP) from Clontech Laboratories (CA, USA). All adenoviruses were amplified in the permissive HEK-293 host cell line (ATCC). Viral particles were purified using the adenoviral purification kit Adeno-X™ (Clontech Laboratories, CA, USA), and the viral title was determined by the end-point dilution assay as described before (Benavides et al. 2005). Astrocytes were infected 2–3 days after subculturing at a multiplicity of infection (MOI) of 20. This MOI rendered high transgenic expression and did not substantially affect cell viability. All experiments involving the use of adenovirus were performed in a P2 biohazard safety level laboratory.

Two-dimensional gel electrophoresis (2DE)

Mouse primary astrocytes were lysed in sample buffer consisting of 7 M urea, 2 M thiourea, 4% CHAPS, 10 mM DTT, 1 mM EDTA, 1 mM phenylmethylsulfonyl fluoride (PMSF) and a mixture of protease and phosphatase

inhibitors (Roche Diagnostics, Mannheim, Germany). After sonication for approximately 15 s, samples were incubated at 21 ± 1°C for 1 h and centrifuged at 14,000*g* at 12°C for 60 min to remove nucleic acids and insoluble material. Desalting was done with Ultrafree-4 centrifugal filter unit (Millipore) and protein content was determined by the Bradford method. 2DE was performed essentially as reported (Yang et al. 2004). Protein samples (0.7 mg) were applied on immobilized pI 3–10 nonlinear gradient strips. Focusing started at 200 V and the voltage was gradually increased to 8,000 V over 31 h at 4 V/min and kept constant for 3 h (approximately 150,000 V h in total). The second-dimensional separation was performed on 9–16% gradient SDS–polyacrylamide gels. After protein fixation for 12 h in 50% methanol and 10% acetic acid, gels were stained with colloidal Coomassie Blue (Novex, San Diego, CA, USA) for 8 h. Excess of dye was washed out with distilled water. Molecular masses were determined by running standard protein markers (Bio-Rad Laboratories, Hercules, CA, USA) covering the range from 10 to 250 kDa. pI values were used as given by the supplier of the immobilized pH gradient strips (Amersham Bioscience).

Quantification of protein spots

Protein spots were outlined automatically and then verified visually. The Proteomweaver software (Definiens, Munich, Germany) was used for image quantification. Protein amount was calculated as spot volume and expressed as percentage of total volume of spots in each 2DE gel. Spots differently expressed after PKCε overexpression were isolated for further analysis.

Sample preparation for mass spectrometry and analysis of peptides by nano-LC–ESI-MS/MS (High Capacity Ion Trap, HCT)

Protein spots identified were manually excised and placed into 0.5 mL LoBind Eppendorf tubes. In-gel digestion and sample preparation for HCT analysis were performed as described before (Sunyer et al. 2008). Gel plugs were washed with 10 mM ammonium bicarbonate and 50% acetonitrile in 10 mM ammonium bicarbonate repeatedly. Addition of 100% acetonitrile resulted in gel shrinking and the shrunk gel plugs were then SpeedVac dried in a SpeedVac Concentrator 5301 (Eppendorf, Germany). The dried gel pieces were re-swollen and in-gel digested overnight at 37°C with 40 ng/μL trypsin (Promega, Madison, WI, USA) in digestion buffer containing 5 mM Octyl β-D-glucopyranoside (OGP) and 10 mM ammonium bicarbonate. Peptide extraction was performed with 20 μL of 1% trifluoroacetic acid (TFA) in 5 mM OGP for 30 min, and subsequently with 0.1% TFA in 4% acetonitrile for 30 min. The extracted peptides were pooled for HCT analysis (a total of 40 μL). The HPLC used was a biocompatible Ultimate 3000 system (Dionex Corporation, Sunnyvale, CA) equipped with a Pep-Map100 C-18 trap column (300 μm × 5 mm) and PepMap100 C-18 analytic column (75 μm × 150 mm). The gradient was (A = 0.1% formic acid in water, B = 0.08% formic acid in acetonitrile) 4–30% B from 0 to 105 min, 80% B from 105 to 110 min, 4% B from 110 to 125 min. The flow rate was 300 nL/min from 0 to 12 min, 75 nL/min from 12 to 105 min, 300 nL/min from 105 to 125 min. An HCT ultra PTM discover system (Bruker Daltonics, Bremen, Germany) was used to record peptide spectra over the mass range of m/z 350–1,500, and MS/MS spectra in information-dependent data acquisition over the mass range of m/z 100–2,800. An active exclusion of 0.4 min after two spectra was used to detect low-abundance peptides. The voltage between ion spray tip and spray shield was set to 1,100 V. Drying nitrogen gas was heated to 170°C and the flow rate was 10 L/min. The collision energy was set automatically according to the mass and charge state of the peptides chosen for fragmentation. Multiple charged peptides were chosen for MS/MS experiments due to their good fragmentation characteristics. MS/MS spectra were interpreted and peak lists were generated by DataAnalysis 3.4 (Bruker Daltonics, Bremen, Germany). Searches were done by using the MASCOT 2.2.04 (Matrix Science, London, UK) against latest UniProtKB database for protein identification. Searching parameters were set as follows: enzyme selected as trypsin with two maximum missing cleavage sites, species limited to mouse, 0.2 Da for MS/MS tolerance, fixed modification of carbamidomethyl and variable modification of methionine oxidation and phosphorylation (Tyr, Thr and Ser). Positive protein identifications were based on a significant MOWSE score. After protein identification, an error-tolerant search was done to detect unspecific cleavage and unassigned modifications. Protein identification and modification information returned from MASCOT were manually inspected and filtered.

Western blot analysis

Cell lysates were loaded onto SDS–polyacrylamide gels, electrophoresed and subsequently transferred to polyvinylidene fluoride membranes (Pall Corporation, Ann Arbor, MI, USA) as described previously (Perez-Ortiz et al. 2004). Protein concentration was measured by the Bradford assay (Bio-Rad, Hercules, CA, USA). Membranes were incubated with a primary antibody for α-B-crystallin (1:5,000; Acris antibodies GmbH, Germany) or HSP60 (1:1,000; Assay designs, Ann Arbor, MI, USA), followed by a mouse peroxidase-conjugated secondary antibody according to a protocol as given by the supplier

(GE Healthcare, UK). An enhanced chemiluminescence system was used for visualization.

Analysis of gene expression by reverse transcription followed by quantitative PCR (RT-PCR)

Total RNA was obtained with the Trizol Reagent (Invitrogen, Carlsbad, CA, USA) following the manufacturer's protocol. The isolated RNA was subsequently treated with DNase (Promega, Madison, WI, USA) to remove any contaminating genomic DNA, and the integrity of RNA was checked by running an aliquot in an agarose gel. Reverse transcription was performed using 2 μg of DNase-treated RNA in 100 μL of reaction volume containing 1× RT Buffer (Applied BioSystems, Carlsbad, CA, USA), 5.5 mM $MgCl_2$, 500 μM dNTPs, 2.5 μM random hexamers, 0.4 U/μL RNase inhibitor, and 1.25 U/μL MultiScribe Reverse Transcriptase. Reaction was performed in a thermal cycler as follows: 25°C for 10 min, 48°C for 30 min and 95°C for 5 min. Samples were then kept at −20°C until utilization.

HSP60 and α-B-crystallin expressions were analysed by quantitative PCR using an ABIPrism 7000 Sequence Detection System (Applied Biosystem). cDNA (2 μL of reverse transcription product) was amplified using SYBR® Green PCR Master Mix (Applied Biosystems) in the presence of primer oligonucleotides specific for HSP60, α-B-crystallin or GAPDH. The PCR conditions were: 95°C for 10 min, followed by 40 cycles consisting of 95°C for 15 s and 60°C for 1 min. Quantification was performed by the comparative cycle threshold method (Livak and Schmittgen 2001), using the GAPDH expression level as internal control. Primers for all target sequences (Table 1) were designed using the computer Primer Express software program provided with the 7000 Sequence Detection System (Applied Biosystems).

Statistical analysis

Protein and mRNA expression values in proteomics, Western blot or RT-PCR experiments are expressed as mean ± standard deviation (SD). Unpaired Student's *t* test (Sunyer et al. 2007) was used for statistical analysis of differences between the CA-PKCε-treated and control groups in all experiments. Spot differences in Proteomweaver analysis were considered significant at $p < 0.05$. Statistical significance of Western blot and RT-PCR quantifications are referred by asterisks ($*p < 0.05$; $**p < 0.01$).

Table 1 Oligonucleotide primer pairs used for HSP60, α-B-crystallin and GAPDH quantification

Name	Sequence
HSP60-F	5′-CACAGTCCTTCGCCAGATGAG-3′
HSP60-R	5′-TGGCATAGGCCCGAGTGA-3′
α-B-crystallin-F	5′-CCAACCGACTCTGCATTCATC-3′
α-B-crystallin-R	5′-GGGCGCCGGATCCA-3′
GAPDH-F	5′-CATCTTCTTGTGCAGTGCCAG-3′
GAPDH-R	5′-CACCGACCTTCACCATTTTGT-3′

Results and discussion

PKCε induces astrocyte stellation

Our previous findings suggest that the astrocyte activation program triggered by PKCε affects multiple cellular pathways. We demonstrated that PKCε induces the expression of voltage-gated calcium channels that may affect a broad range of calcium-dependent processes (Burgos et al. 2007b) and also regulates cytoskeletal components implicated in cell morphology determination (Burgos et al. 2007a). Inspired by the fact that astrocyte activation has a profound impact on neuronal survival in neuroinflammatory pathologies, here we use a proteomics approach to disclose novel PKCε molecular targets.

Our first step to identify proteins regulated by PKCε was to set primary astrocyte cultures from mice cortex. We have previously shown that this cellular system responds to PKCε. To analyse the effects of PKCε in the present experiments, astrocyte cultures were infected with an adenovirus expressing a constitutively active form of PKCε (AdCA-PKCε). Western blot analysis demonstrated that AdCA-PKCε infection triggers a high CA-PKCε expression (Fig. 1a). Moreover, PKCε induction was associated to a dramatic change in morphology. Astrocytes developed long cell processes clearly visible in phase-contrast images and similar to those found in reactive astrocytes (Fig. 1b). Complementary immunofluorescence staining showed that PKCε overexpression by adenoviral infection is effective in most astrocytes within the culture (over 90%). Control cultures were infected with an adenovirus expressing β-galactosidase (Adβ-GAL) or green fluorescent protein (AdGFP). No changes were observed after infection with any control adenovirus, implying that the morphological transformation observed depends on the expression of PKCε, and not on the adenoviral infection itself.

Analysis of indicated spots

Regulation of protein expression by PKCε in primary astrocyte cultures was analysed by proteomics technique. To examine proteome differences between CA-PKCε-infected astrocytes and β-GAL-expressing controls,

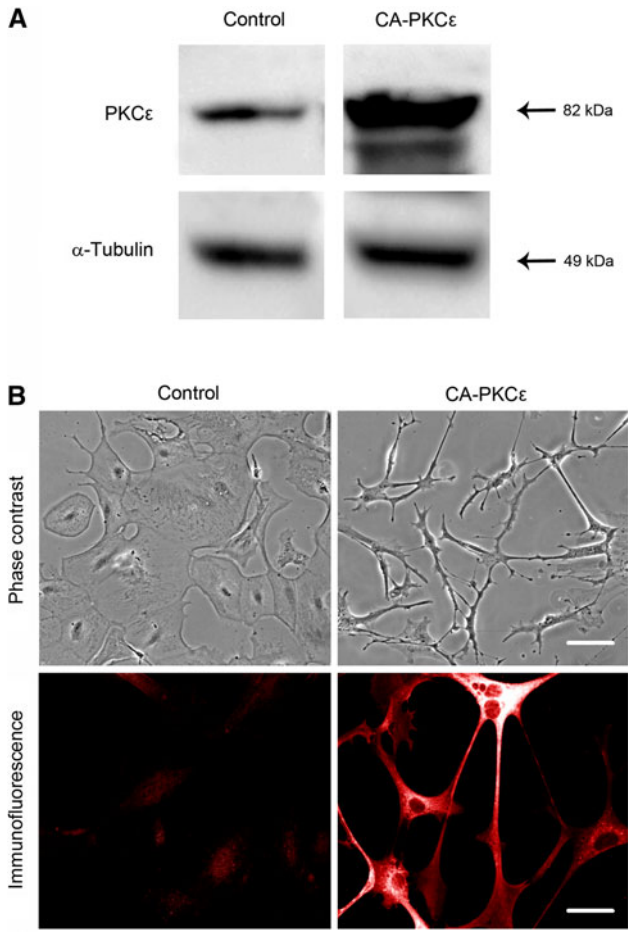

Fig. 1 PKCε induces a reactive morphology in astrocytes. Astrocyte cultures were transduced with an adenoviral construct expressing a constitutively active form of PKCε (AdCA-PKCε) whereas controls were exposed to adenovirus producing β-GAL (Adβ GAL). **a** After 72 h PKCε expression in AdCA-PKCε and Adβ GAL cultures was studied by Western blot analysis. Detection of α-tubulin was included as a loading control. **b** Cultures were processed to evaluate astrocyte morphology by phase-contrast microscopy (*upper panels*) or PKCε expression by immunofluorescence (*lower panels*). *Scale bar* corresponds to 100 and 50 μm (*upper* and *lower images* respectively). Data shown are representative of at list six independent experiments. PKCε overexpression triggers a dramatic morphological change inducing the elongation of cell processes which is characteristic of reactive astrocytes

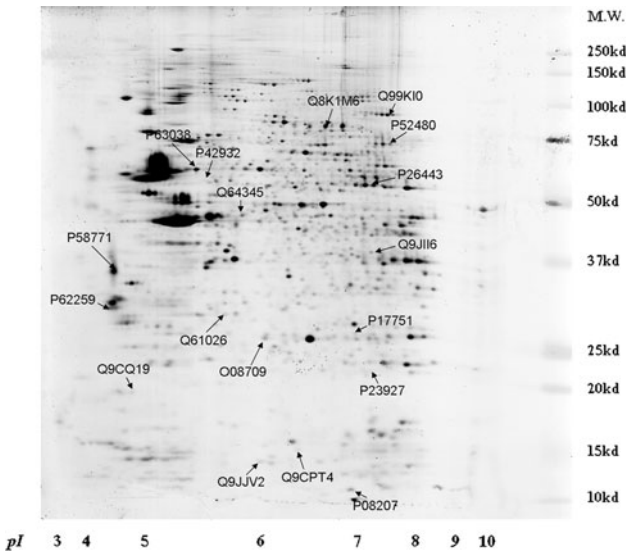

Fig. 2 2DE image of primary astrocyte cultures. Proteins from AdCA-PKCε-infected astrocytes and Adβ GAL-infected controls were extracted and separated on an immobilized pH 3–10 non-linear gradient strip followed by separation on a 9–16% polyacrylamide gradient. Gels were stained with Coomassie Blue and spots were subjected to densitometric analysis using Proteomweaver software. *Spots* highlighted correspond to differentially expressed proteins identified by nano-LC–ESI-MS/MS. Accession numbers for these proteins are provided. Unpaired Student's *t* test was used for statistical analysis

proteins were extracted and separated on 2DE (Fig. 2). Densitometric analysis using Proteomweaver software was applied to 549 spots. The unpaired Student's *t* test detected statistically significant differences among controls and CA-PKCε overexpressing astrocytes in 18 spots. All differentially expressed spots were subjected to nano-LC–ESI-MS/MS for protein identification (Supplementary Table 1). Differences in protein expression are shown in Table 2.

Although proteins identified as PKCε targets in our study have heterogeneous functions, they can be classified in to chaperones, cytoskeletal, metabolism-related and antioxidant proteins. In addition, both upregulated and downregulated proteins were found. Thus, α-B-crystallin, 60 kDa heat shock protein (HSP60), 14-3-3 ε, pyruvate kinase isozymes M1/M2, T-complex protein 1θ and UPF0556 protein C19orf10 homologue showed significantly higher expression in the CA-PKCε-infected group; whereas expression of alcohol dehydrogenase (NADP+), dynamin-1-like-protein, glutamate dehydrogenase 1 (mitochondrial), interferon-induced protein with tetratricopeptide repeats 3, myosin regulatory light polypeptide 9, peroxiredoxin-6, platelet-activating factor acetylhydrolase IB β, profilin-2, triosephosphate isomerase, tropomyosin α-1 chain and protein S100-A10 were significantly decreased after CA-PKCε induction.

The regulation of α-B-crystallin and HSP60 in response to PKCε overexpression was further analysed by Western blotting. Control and AdCA-PKCε-treated samples were incubated with HSP60 and α-B-crystallin specific antibodies. Both HSP60 and α-B-crystallin were significantly increased in CA-PKCε-overexpressing astrocytes (44 and 50% respectively), which confirmed proteomics results (Fig. 3a). To assess whether changes in protein levels are the consequence of transcriptional or post-transcriptional mechanisms, mRNA levels were measured by RT-PCR with oligonucleotides designed to specifically amplify HSP60 or α-B-crystallin. Whereas expression of α-B-crystallin mRNA

Table 2 Quantification of proteins after 2DE analysis and identification by nano-LC–ESI-MS/MS

Accession number	Name	Adβ-gal-infected astrocytes	AdCA-PKCε-infected astrocytes
P62259	14-3-3 ε	2.27 ± 0.90	5.17 ± 1.43
P63038	60 kDa heat shock protein mitochondrial	1.88 ± 0.36	2.71 ± 0.51
Q99KI0	Aconitate hydratase mitochondrial	0.90 ± 0.11	1.28 ± 0.19
Q9JII6	Alcohol dehydrogenase [NADP+]	0.43 ± 0.05	0.33 ± 0.08
P23927	α-B-crystallin	0.35 ± 0.12	0.58 ± 0.11
Q8K1M6	Dynamin-1-like protein	1.51 ± 0.28	1.10 ± 0.12
P26443	Glutamate dehydrogenase 1 mitochondrial	1.99 ± 0.20	1.51 ± 0.30
Q64345	Interferon-induced protein with tetratricopeptide repeats 3	0.59 ± 0.18	0.36 ± 0.05
Q9CQ19	Myosin regulatory light polypeptide 9	0.40 ± 0.047	0.25 ± 0.11
O08709	Peroxiredoxin-6	0.87 ± 0.18	0.55 ± 0.12
Q61206	Platelet-activating factor acetylhydrolase IB β	0.36 ± 0.03	0.30 ± 0.02
Q9JJV2	Profilin-2	0.43 ± 0.01	0.30 ± 0.08
P52480	Pyruvate kinase isozymes M1/M2	0.63 ± 0.20	0.83 ± 0.33
P42932	T-complex protein 1 θ	0.33 ± 0.04	0.46 ± 0.07
P17751	Triosephosphate isomerase	0.40 ± 0.05	0.33 ± 0.02
P58771	Tropomyosin α-1 chain	5.84 ± 0.49	3.85 ± 0.82
Q9CPT4	UPF0556 protein C19orf10 homolog	0.22 ± 0.04	0.30 ± 0.02
P08207	Protein S100-A10	1.03 ± 0.03	0.85 ± 0.12

Relative protein expression (mean ± SD) shown is the result of Proteomweaver software-assisted quantification. Only proteins presenting a statistically different expression between AdCA-PKCε- and Adβ-gal-infected astrocytes ($p < 0.05$ Student's t test) are listed

was significantly increased by CA-PKCε, we found no evidence of effects on HSP60 mRNA (Fig. 3b). This result indicates different levels of regulation for the proteins studied.

Stress proteins identified as PKCε targets play roles in neuroinflammation

Our experiments show increased expression of several specific chaperone and chaperone-related (chaperonin) proteins in astrocytes as a consequence of PKCε overexpression. These proteins are α-B-crystallin, HSP60, the subunit theta of T-complex protein 1 (TCP-1) and 14-3-3 ε. The expression of chaperones is generally constitutive, as they regulate fundamental cellular process affecting protein folding, sorting, degradation, assembly into complexes and resolubilization of aggregates (Chen et al. 2006). Interestingly, chaperones have a particularly high expression in response to deleterious cell environments that alter protein folding, and are often markedly upregulated under conditions of cellular stress including inflammation. In consequence, the regulation of stress proteins by PKCε uncovered by our experiments may be related with the function of chaperones as inflammatory mediators. In fact, chaperones are known to influence inflammatory signalling pathways (van Noort 2008). Furthermore, since astrocytes are cells with immune functions and our previous data indicate that PKCε induces astrocyte activation, the evidence gathered here suggests the involvement of chaperones in the inflammatory signalling cascades controlled by PKCε that are related to astrogliosis. Evidence supporting this notion for specific PKCε-regulated chaperones is discussed below.

α-B-crystallin

Our experiments reveal a substantial upregulation of α-B-crystallin in PKCε-stimulated astrocytes. Proteomics data was confirmed through complementary Western blot analysis. Moreover, RT-PCR showed that regulation of α-B-crystallin by PKCε implicates changes at the mRNA level. The chaperone protein α-B-crystallin is known to increase in the brain in cellular stress conditions, and often in neurological diseases related to aggregation of misfolded proteins. In agreement with our results, α-B-crystallin expression is particularly high in reactive astrocytes both in diseased human brain (Iwaki et al. 1992) and in animal models of neuropathology, such as middle cerebral artery occlusion (Piao et al. 2005), tauopathies (Dabir et al. 2004), kainate-mediated excitotoxicity (Che et al. 2001) and Parkinson disease (Renkawek et al. 1999). Moreover, α-B-crystallin upregulation in glial cells has been shown protective in Huntington's disease by suppression of α-synuclein aggregates (Wang et al. 2008). In the same line, CNS inflammation and demyelination in experimental autoimmune encephalomyelitis (EAE) was aggravated in a

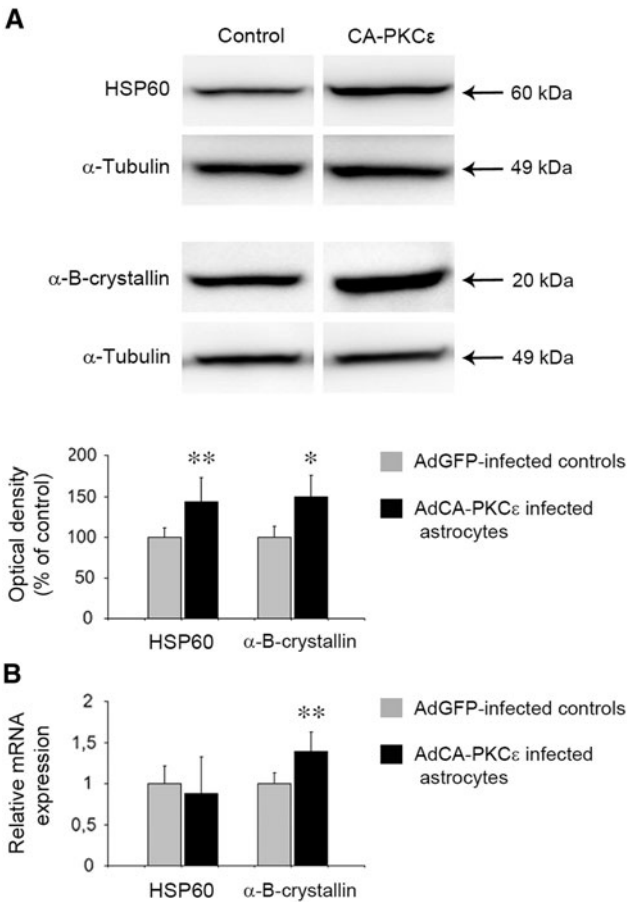

Fig. 3 Western blot and RT-PCR analysis of HSP60 and α-B-crystallin regulation by PKCε. Astrocyte cultures overexpressing CA-PKCε or GFP (controls) were compared. **a** Protein extracts were processed for immunoblotting with specific antibodies to HSP60 or α-B-crystallin and detection of α-tubulin was included as a loading control. Western blot shown is representative of four independent experiments. Optical density values in the densitometric analysis are expressed as percentage of Adβ GAL-infected controls. **b** RNA obtained from astrocytes overexpressing CA-PKCε or GFP was subjected to RT-PCR. GAPDH expression was used as internal control. Numeric values are presented as increments over control astrocytes. Results are expressed as mean ± standard deviation (SD) of nine experiments performed using three independent astrocyte cultures. $*p < 0.05$ and $**p < 0.01$ vs. controls. Whereas both HSP60 and α-B-crystallin proteins are significantly increased in cells overexpressing CA-PKCε only α-B-crystallin mRNA was upregulated by PKCε

mouse model in which astrocytes lacked α-B-crystallin expression (Ousman et al. 2007). Therefore, there is evidence to sustain the hypothesis that PKCε-controlled signalling pathways in which α-B-crystallin is implicated might be neuroprotective. On the other hand, although this is the first report associating PKCε to α-B-crystallin, previous work has linked PKC activation to the regulation of this chaperone. In this regard, PKC-induced activation of p38 has been shown responsible for α-B-crystallin phosphorylation (Launay et al. 2006); and α-B-crystallin is a PKCδ target in retinas of type 2-diabetes patients (Kim et al. 2007).

HSP60

HSP60 belongs to a particular family of chaperone proteins named chaperonins. HSP60 is known to act as a potent stimulator of innate immunity (Quintana and Cohen 2008), and to induce the release of inflammatory mediators, such as IL-6 in mouse adipocytes (Gulden et al. 2008). Conversely, proinflammatory cytokines have been reported to enhance HSP60 expression in astrocytes (Bajramovic et al. 2000), inspiring the idea that HSP60 play a role in the pathogenesis of autoimmune diseases. In accordance with the implication of HSP60 in neuroinflammatory pathologies, data collected here associate HSP60 expression with PKCε-induced astrocyte activation. Our initial proteomic experiments were confirmed by Western blotting. Besides, RT-PCR analysis added complementary evidence suggesting that HSP60 regulation by PKCε takes place at the posttranscriptional level. Further supporting the role of HSP60 in PKCε signalling, a previous report showed that HSP60 overexpression in stressing conditions can be inhibited by PKC blockers (Chen et al. 2006).

14-3-3 ε

14-3-3 is a highly conserved family of adapter proteins (Bridges and Moorhead 2005) that regulates the function of a large number of target proteins by restricting their subcellular location, modulating their catalytic activity and protecting them from dephosphorylation or proteolysis. In consequence, 14-3-3 chaperones control signalling pathways involved in cell differentiation, proliferation, transformation and apoptosis (Berg et al. 2003). The proteome analysis shown here detects that PKCε enhances the expression of the epsilon subtype specifically. Previous reports have shown upregulation of 14-3-3 ε in brains of patients with Alzheimer disease and Down syndrome (Fountoulakis et al. 1999). Moreover, in accordance with our observations, expression of 14-3-3 ε is increased in reactive astrocytes present in models of brain lesion, such as hippocampal denervation in mouse (Sihlbom et al. 2007). It is also associated to astrocyte activation in human neuropathologies including multiple sclerosis (Satoh et al. 2004) and cerebrovascular ischemia (Kawamoto et al. 2006). Therefore, the finding that 14-3-3 ε is under PKCε control further supports the involvement of this kinase in astrogliosis and pathogenesis in the CNS. It is also interesting to note that 14-3-3 proteins can form molecular complexes with HSP60, another protein identified here as a chaperone responsive to PKCε (Satoh et al. 2005).

Metabolic proteins and other enzymes with a putative role in neuroinflammation

Acquisition of the reactive phenotype in astrocytes is associated to profound metabolic changes. Triosephosphate isomerase, alcohol dehydrogenase, aconitate hydratase and pyruvate kinase are a group of proteins related to the cellular metabolism that are altered by PKCε overexpression. Supporting their possible involvement in PKCε-induced astrogliosis, the activity of pyruvate kinase was previously found increased in reactive astrocytes in a model of hypoxia (Marrif and Juurlink 1999), as well as in brains of patients with Alzheimer's disease (Bigl et al. 1999). In addition, peroxiredoxin-6 is a protein belonging to a ubiquitous family of antioxidant enzymes downregulated here by PKCε. Inhibition of this enzyme in lung tumorigenesis was also linked to inflammation (Meier et al. 2007). It is interesting to note that not all enzymatic changes induced by PKCε in our study are supposed to lead to increased inflammation. In this regard, IFN-induced protein with tetratricopeptide repeat 3 is a proinflammatory marker of astrocyte activation decreased after PKCε stimulation. Another protein with enzymatic activity found differentially regulated by proteomics is platelet-activating factor acetyl (PAF) hydrolase (PAF-AH), which catalyzes the degradation of PAF. This factor is a mediator of inflammation in activated leukocytes, further suggesting that at least part of the signalling pathways activated by PKCε in reactive astrocytes may be anti-inflammatory. In agreement with our results, a previous work found decreased PAF-AH after PKC activation with phorbol esters in macrophages (Narahara et al. 2003).

Candidates to mediate astrocyte stellation induced by PKCε

PKCε stimulation induces the growth of cellular processes in the astrocyte activation model used here. This transformation resembles the morphological change observed in reactive astrocytes in damaged brains, and was characterized in our previous work. Thus, we found that PKCε promotes the assembly of actin and tubulin filaments, as well as myosin light chain 2 phosphorylation (Burgos et al. 2007a). In this context, it is meaningful that our proteomic approach was able to identify as PKCε targets several proteins involved in cell shaping. One of them is myosin regulatory light polypeptide 9, a protein that modulates the ATPase activity of myosin heads (Takashima 2009). We found a decrease in the levels of this protein in response to PKCε activation. Other proteins downregulated according to the present proteomic results are: tropomyosin α-1 chain, also related to myosin (Malhotra 1994); dynamin 1-like-protein, involved in endocytosis and vesicular trafficking (Koch et al. 2004), and S100A10 (p11), a member of the S100 protein family that forms a heterotetrameric complex with annexin 2 and regulates intracellular trafficking and protein expression at the cell surface. Besides, S100A10 (p11) can influence the organization of the actin cytoskeleton (Benaud et al. 2004). Another protein identified that also relates to the cytoskeleton is T-complex protein 1 subunit theta (TCP-1 δ). Proteins of the TCP-1 complex belong to the same chaperone family than HSP60, also found here. Interestingly, TCP-1 acts as a cytosolic chaperone implicated in folding of the cytoskeletal proteins actin and tubulin (Dunn et al. 2001), as well as myosin (Srikakulam and Winkelmann 1999). In addition, both HSP60 and TCP-1 show abnormal activity in neuroinflammatory pathologies, such as Alzheimer's disease (Nicolls et al. 2003). All these evidence together underline the remarkable similarities between the functions of the structural proteins detected as PKCε targets, and the actions of PKCε on the cytoskeleton previously described. Then, a plausible hypothesis is that our proteomic analysis has identified several mediators of the cytoskeletal effects of PKCε. Finally, it can also be proposed that these cytoskeleton-associated proteins could be involved in astrocyte stellation linked to astrogliosis.

Conclusions

Even though 2DE is only able to separate highly abundant proteins (around 2,000 out of the 10^4 proteins expressed in a single eukaryotic cell), proteomics has been validated as a potent technique for comparison of proteins differentially expressed among experimental groups (Suder et al. 2009). Thus, despite the fact that the map of proteins under PKCε regulation obtained is not exhaustive, the proteomics approach used here has proven greatly informative and has yielded data that extend to a broad range of protein categories. Moreover, considering that our astrogliosis model by PKCε overexpression may be applied to astrocyte activation in many neuroinflammatory disorders, the results presented in this report may throw light on intracellular pathways common to numerous neuropathologies.

Several classifications of proteins regulated by PKCε could have been applied to attend the diversity of PKCε actions. However, proteins have been finally organized in a way that facilitates understanding the implication of PKCε activation for neuroimmunity. In fact, we found that most proteins identified by proteomics fit naturally within signalling pathways possibly related to immune functions played by astrocytes. In particular, we detected a group of chaperones needed for correct brain function and the expression of which is found altered in association to inflammation. Our findings support the idea that

modulation of astrocytic chaperones by PKCε, as well as metabolic and antioxidant enzymes, favour mainly proinflammatory processes which could be relevant in the context of neurological disorders. Furthermore, the fact that a group of proteins related to the actin and myosin cytoskeleton are identified in this study strengthens the notion that PKCε controls astrocyte morphology, and support our previous findings indicating that PKCε promotes a stellated morphology characteristic of reactive astrocytes associated to neuroinflammation. Overall, the proteomic analysis presented here may contribute to elucidate signalling cascades implicated in astrocyte activation in response to PKCε stimulation, as well as the implication of astrocytes in the progression of neuroinflammatory disorders.

Acknowledgments We thank V. Corrales, G. Rodríguez, P. Alfaro and E. Chantre for technical assistance and A. Samarel for kindly providing AdCA-PKCε and Adβgal. This work has been supported by a SAN06-010 grant from JCCM to P. Tranque and BFU2006-14267, PAI05-017 and PCI-08-0101-8639 to S.C. M. Burgos and N. Fradejas have JCCM fellowships. We are highly indebted to Drs. Berta Sunyer and Wei-Qiang Chen for technical support.

References

Abbott NJ, Revest PA, Romero IA (1992) Astrocyte-endothelial interaction: physiology and pathology. Neuropathol Appl Neurobiol 18:424–433

Agulhon C, Petravicz J, McMullen AB, Sweger EJ, Minton SK, Taves SR, Casper KB, Fiacco TA, McCarthy KD (2008) What is the role of astrocyte calcium in neurophysiology? Neuron 59:932–946

Akita Y (2002) Protein kinase C-epsilon (PKC-epsilon): its unique structure and function. J Biochem 132:847–852

Aksoy E, Goldman M, Willems F (2004) Protein kinase C epsilon: a new target to control inflammation and immune-mediated disorders. Int J Biochem Cell Biol 36:183–188

Bajramovic JJ, Bsibsi M, Geutskens SB, Hassankhan R, Verhulst KC, Stege GJ, de Groot CJ, van Noort JM (2000) Differential expression of stress proteins in human adult astrocytes in response to cytokines. J Neuroimmunol 106:14–22

Benaud C, Gentil BJ, Assard N, Court M, Garin J, Delphin C, Baudier J (2004) AHNAK interaction with the annexin 2/S100A10 complex regulates cell membrane cytoarchitecture. J Cell Biol 164:133–144

Benavides A, Pastor D, Santos P, Tranque P, Calvo S (2005) CHOP plays a pivotal role in the astrocyte death induced by oxygen and glucose deprivation. Glia 52:261–275

Berg D, Holzmann C, Riess O (2003) 14-3-3 proteins in the nervous system. Nat Rev Neurosci 4:752–762

Bigl M, Bruckner MK, Arendt T, Bigl V, Eschrich K (1999) Activities of key glycolytic enzymes in the brains of patients with Alzheimer's disease. J Neural Transm 106:499–511

Blasko I, Stampfer-Kountchev M, Robatscher P, Veerhuis R, Eikelenboom P, Grubeck-Loebenstein B (2004) How chronic inflammation can affect the brain and support the development of Alzheimer's disease in old age: the role of microglia and astrocytes. Aging Cell 3:169–176

Bridges D, Moorhead GB (2005) 14-3-3 proteins: a number of functions for a numbered protein. Sci STKE 296:re10

Brown AM, Ransom BR (2007) Astrocyte glycogen and brain energy metabolism. Glia 55:1263–1271

Buffo A, Rolando C, Ceruti S (2010) Astrocytes in the damaged brain: molecular and cellular insights into their reactive response and healing potential. Biochem Pharmacol 79:77–89

Burgos M, Calvo S, Molina F, Vaquero CF, Samarel A, Llopis J, Tranque P (2007a) PKCepsilon induces astrocyte stellation by modulating multiple cytoskeletal proteins and interacting with Rho A signalling pathways: implications for neuroinflammation. Eur J Neurosci 25:1069–1078

Burgos M, Pastor MD, Gonzalez JC, Martinez-Galan JR, Vaquero CF, Fradejas N, Benavides A, Hernandez-Guijo JM, Tranque P, Calvo S (2007b) PKCepsilon upregulates voltage-dependent calcium channels in cultured astrocytes. Glia 55:1437–1448

Bush TG, Puvanachandra N, Horner CH, Polito A, Ostenfeld T, Svendsen CN, Mucke L, Johnson MH, Sofroniew MV (1999) Leukocyte infiltration neuronal degeneration and neurite outgrowth after ablation of scar-forming reactive astrocytes in adult transgenic mice. Neuron 23:297–308

Castrillo A, Pennington DJ, Otto F, Parker PJ, Owen MJ, Bosca L (2001) Protein kinase Cepsilon is required for macrophage activation and defense against bacterial infection. J Exp Med 194:1231–1242

Che Y, Piao CS, Han PL, Lee JK (2001) Delayed induction of alpha B-crystallin in activated glia cells of hippocampus in kainic acid-treated mouse brain. J Neurosci Res 65:425–431

Chen HB, Chan YT, Hung AC, Tsai YC, Sun SH (2006) Elucidation of ATP-stimulated stress protein expression of RBA-2 type-2 astrocytes: ATP potentiate HSP60 and Cu/Zn SOD expression and stimulates pI shift of peroxiredoxin II. J Cell Biochem 97:314–326

Chung YH, Shin CM, Kim MJ, Cha CI (2001) Enhanced expression of L-type Ca2+ channels in reactive astrocytes after ischemic injury in rats. Neurosci Lett 302:93–96

Dabir DV, Trojanowski JQ, Richter-Landsberg C, Lee VM, Forman MS (2004) Expression of the small heat-shock protein alphaB-crystallin in tauopathies with glial pathology. Am J Pathol 164:155–166

Diez-Vives C, Gay M, Garcia-Matas S, Comellas F, Carrascal M, Abian J, Ortega-Aznar A, Cristofol R, Sanfeliu C (2009) Proteomic study of neuron and astrocyte cultures from senescence-accelerated mouse SAMP8 reveals degenerative changes. J Neurochem 111:945–955

Dong Y, Benveniste EN (2001) Immune function of astrocytes. Glia 36:180–190

Dowell JA, Johnson JA, Li L (2009) Identification of astrocyte secreted proteins with a combination of shotgun proteomics and bioinformatics. J Proteome Res 8:4135–4143

Dunn AY, Melville MW, Frydman J (2001) Review: cellular substrates of the eukaryotic chaperonin TRiC/CCT. J Struct Biol 135:176–184

Egnaczyk GF, Pomonis JD, Schmidt JA, Rogers SD, Peters C, Ghilardi JR, Mantyh PW, Maggio JE (2003) Proteomic analysis of the reactive phenotype of astrocytes following endothelin-1 exposure. Proteomics 3:689–698

Faulkner JR, Herrmann JE, Woo MJ, Tansey KE, Doan NB, Sofroniew MV (2004) Reactive astrocytes protect tissue and preserve function after spinal cord injury. J Neurosci 24: 2143–2155

Fountoulakis M, Cairns N, Lubec G (1999) Increased levels of 14-3-3 gamma and epsilon proteins in brain of patients with Alzheimer's disease and Down syndrome. J Neural Transm Suppl 57:323–335

Giaume C, Kirchhoff F, Matute C, Reichenbach A, Verkhratsky A (2007) Glia: the fulcrum of brain diseases. Cell Death Differ 14:1324–1335

Gulden E, Mollerus S, Bruggemann J, Burkart V, Habich C (2008) Heat shock protein 60 induces inflammatory mediators in mouse adipocytes. FEBS Lett 582:2731–2736

Heidkamp MC, Bayer AL, Martin JL, Samarel AM (2001) Differential activation of mitogen-activated protein kinase cascades and apoptosis by protein kinase C epsilon and delta in neonatal rat ventricular myocytes. Circ Res 89:882–890

Hertz L, Dringen R, Schousboe A, Robinson SR (1999) Astrocytes: glutamate producers for neurons. J Neurosci Res 57:417–428

Iwaki T, Wisniewski T, Iwaki A, Corbin E, Tomokane N, Tateishi J, Goldman JE (1992) Accumulation of alpha B-crystallin in central nervous system glia and neurons in pathologic conditions. Am J Pathol 140:345–356

Karwoski CJ, Lu HK, Newman EA (1989) Spatial buffering of light-evoked potassium increases by retinal Muller (glial) cells. Science 244:578–580

Kawamoto Y, Akiguchi I, Tomimoto H, Shirakashi Y, Honjo Y, Budka H (2006) Upregulated expression of 14–3-3 proteins in astrocytes from human cerebrovascular ischemic lesions. Stroke 37:830–835

Keene SD, Greco TM, Parastatidis I, Lee SH, Hughes EG, Balice-Gordon RJ, Speicher DW, Ischiropoulos H (2009) Mass spectrometric and computational analysis of cytokine-induced alterations in the astrocyte secretome. Proteomics 9:768–782

Kim YH, Choi MY, Kim YS, Han JM, Lee JH, Park CH, Kang SS, Choi WS, Cho GJ (2007) Protein kinase C delta regulates anti-apoptotic alphaB-crystallin in the retina of type 2 diabetes. Neurobiol Dis 28:293–303

Koch A, Schneider G, Luers GH, Schrader M (2004) Peroxisome elongation and constriction but not fission can occur independently of dynamin-like protein 1. J Cell Sci 117:3995–4006

Laird MD, Vender JR, Dhandapani KM (2008) Opposing roles for reactive astrocytes following traumatic brain injury. Neurosignals 16:154–164

Launay N, Goudeau B, Kato K, Vicart P, Lilienbaum A (2006) Cell signaling pathways to alphaB-crystallin following stresses of the cytoskeleton. Exp Cell Res 312:3570–3584

Livak KJ, Schmittgen TD (2001) Analysis of relative gene expression data using real-time quantitative PCR and the 2(-Delta Delta C(T)) Method. Methods 25:402–408

Malhotra A (1994) Role of regulatory proteins (troponin-tropomyosin) in pathologic states. Mol Cell Biochem 135:43–50

Maragakis NJ, Rothstein JD (2006) Mechanisms of disease: astrocytes in neurodegenerative disease. Nat Clin Pract Neurol 2:679–689

Marrif H, Juurlink BH (1999) Astrocytes respond to hypoxia by increasing glycolytic capacity. J Neurosci Res 57:255–260

Meier BW, Gomez JD, Kirichenko OV, Thompson JA (2007) Mechanistic basis for inflammation and tumor promotion in lungs of 2,6-di-tert-butyl-4-methylphenol-treated mice: electrophilic metabolites alkylate and inactivate antioxidant enzymes. Chem Res Toxicol 20:199–207

Myung JK, Shim KS, Li L, Höger H, Lubec G (2009) Developmental brain protein level changes in the C57BL/6 J mouse. J Proteome Res 8:1207–1219

Narahara H, Kawano Y, Nasu K, Yoshimatsu J, Johnston JM, Miyakawa I (2003) Platelet-activating factor inhibits the secretion of platelet-activating factor acetylhydrolase by human decidual macrophages. J Clin Endocrinol Metab 88:6029–6033

Nicolls MR, D'Antonio JM, Hutton JC, Gill RG, Czwornog JL, Duncan MW (2003) Proteomics as a tool for discovery: proteins implicated in Alzheimer's disease are highly expressed in normal pancreatic islets. J Proteome Res 2:199–205

Ousman SS, Tomooka BH, van Noort JM, Wawrousek EF, O'Connor KC, Hafler DA, Sobel RA, Robinson WH, Steinman L (2007) Protective and therapeutic role for alphaB-crystallin in autoimmune demyelination. Nature 448:474–479

Perez-Ortiz JM, Tranque P, Vaquero CF, Domingo B, Molina F, Calvo S, Jordan J, Cena V, Llopis J (2004) Glitazones differentially regulate primary astrocyte and glioma cell survival. Involvement of reactive oxygen species and peroxisome proliferator-activated receptor-gamma. J Biol Chem 279:8976–8985

Peyrl A, Krapfenbauer K, Slavc I, Strobel T, Lubec G (2003) Proteomic characterization of the human cortical neuronal cell line HCN-2. J Chem Neuroanat 26:171–178

Piao CS, Kim SW, Kim JB, Lee JK (2005) Co-induction of alphaB-crystallin and MAPKAPK-2 in astrocytes in the penumbra after transient focal cerebral ischemia. Exp Brain Res 163:421–429

Premkumar LS, Ahern GP (2000) Induction of vanilloid receptor channel activity by protein kinase C. Nature 408:985–990

Quintana FJ, Cohen IR (2008) HSP60 speaks to the immune system in many voices. Novartis Found Symp 291:101–111

Rakic P (1972) Mode of cell migration to the superficial layers of fetal monkey neocortex. J Comp Neurol 145:61–83

Renkawek K, Stege GJ, Bosman GJ (1999) Dementia gliosis and expression of the small heat shock proteins hsp27 and alpha B-crystallin in Parkinson's disease. Neuroreport 10:2273–2276

Rolls A, Shechter R, Schwartz M (2009) The bright side of the glial scar in CNS repair. Nat Rev Neurosci 10:235–241

Satoh J, Yamamura T, Arima K (2004) The 14-3-3 protein epsilon isoform expressed in reactive astrocytes in demyelinating lesions of multiple sclerosis binds to vimentin and glial fibrillary acidic protein in cultured human astrocytes. Am J Pathol 165:577–592

Satoh J, Onoue H, Arima K, Yamamura T (2005) The 14-3-3 protein forms a molecular complex with heat shock protein Hsp60 and cellular prion protein. J Neuropathol Exp Neurol 64:858–868

Sihlbom C, Wilhelmsson U, Li L, Nilsson CL, Pekny M (2007) 14-3-3 expression in denervated hippocampus after entorhinal cortex lesion assessed by culture-derived isotope tags in quantitative proteomics. J Proteome Res 6:3491–3500

Skaper SD (2007) The brain as a target for inflammatory processes and neuroprotective strategies. Ann N Y Acad Sci 1122:23–34

Srikakulam R, Winkelmann DA (1999) Myosin II folding is mediated by a molecular chaperonin. J Biol Chem 274:27265–27273

Suder P, Bodzon-Kulakowska A, Mak P, Bierczynska-Krzysik A, Daszykowski M, Walczak B, Lubec G, Kotlinska JH, Silberring J (2009) The proteomic analysis of primary cortical astrocyte cell culture after morphine administration. J Proteome Res 8:4633–4640

Sunyer B, Patil S, Frischer C, Hoger H, Selcher J, Brannath W, Lubec G (2007) Strain-dependent effects of SGS742 in the mouse. Behav Brain Res 181:64–75

Sunyer B, Diao WF, Kang SU, An G, Boddul S, Lubec G (2008) Cognitive enhancement by SGS742 in OF1 mice is linked to specific hippocampal protein expression. J Proteome Res 7:5237–5253

Takashima S (2009) Phosphorylation of myosin regulatory light chain by myosin light chain kinase and muscle contraction. Circ J 73:208–213

Tan SL, Parker PJ (2003) Emerging and diverse roles of protein kinase C in immune cell signalling. Biochem J 376:545–552

Tsacopoulos M, Magistretti PJ (1996) Metabolic coupling between glia and neurons. J Neurosci 16:877–885

van Noort JM (2008) Stress proteins in CNS inflammation. J Pathol 214:267–275

Wang J, Bright R, Mochly-Rosen D, Giffard RG (2004) Cell-specific role for epsilon- and betaI-protein kinase C isozymes in protecting cortical neurons and astrocytes from ischemia-like injury. Neuropharmacology 47:136–145

Wang J, Martin E, Gonzales V, Borchelt DR, Lee MK (2008) Differential regulation of small heat shock proteins in transgenic

mouse models of neurodegenerative diseases. Neurobiol Aging 29:586–597

Westenbroek RE, Bausch SB, Lin RC, Franck JE, Noebels JL, Catterall WA (1998) Upregulation of L-type Ca2+ channels in reactive astrocytes after brain injury hypomyelination and ischemia. J Neurosci 18:2321–2334

Yang JW, Czech T, Lubec G (2004) Proteomic profiling of human hippocampus. Electrophoresis 25:1169–1174

Yang JW, Suder P, Silberring J, Lubec G (2005) Proteome analysis of mouse primary astrocytes. Neurochem Int 47:159–172